Available online at www.scholarsresearchlibrary.com

Scholars Research Library

Der Pharmacia Lettre, 2016, 8 (4):96-107
(http://scholarsresearchlibrary.com/archive.html)

ISSN 0975-5071
USA CODEN: DPLEB4

Evaluation of corrosion inhibition of mild steel in 1.0 M HCl by Sulfathiazole: Experimental and theoretical studies

M. Saadouni[1], M. Larouj[2], R. Salghi[3*], H. Lgaz[2,3], S. Jodeh[4*], M. Zougagh[5,6] and A. Souizi[1]

[1]*Laboratory of Organic, Organometallic and Theoretical Chemistry, Faculty of Science, Ibn Tofaïl University, 14000 Kenitra, Morocco*
[2]*Laboratory Separation Processes, Faculty of Science, University IbnTofail PO Box 242, Kenitra, Morocco*
[3]*Laboratory of Applied Chemistry and Environment, ENSA, Université Ibn Zohr, PO Box 1136, 80000 Agadir, Morocco*
[4]*Department of Chemistry, An-Najah National University, P. O. Box 7, Nablus, Palestine*
[5]*Regional Institute for Applied Chemistry Research, IRICA, E-13004, Ciudad Real, Spain*
[6]*Castilla-La Mancha Science and Technology Park, E-02006, Albacete, Spain*

ABSTRACT

*The inhibition effect of sulfathiazole (**STZ**) on the corrosion inhibition of mild steel in 1.0 M HCl solution was studied by polarization, EIS, weight loss measurements and quantum chemical calculation. It was found that the inhibitor was effective and the inhibition efficiency was significantly increased with increasing concentration. Polarization curves revealed that the used inhibitor represent mixed-type inhibitor. Adsorption of the inhibitor led to a reduction in the double layer capacitance and an increase in the charge transfer resistance, and was found also to obey Langmuir isotherm. A good correlation between theoretical data and experimental data has been obtained.*

Keywords: Corrosion inhibition; DFT; Sulfathiazole; HCl; EIS, Polarization

---

INTRODUCTION

Corrosion inhibitors are of great practical importance, being extensively employed in minimizing metallic waste in engineering materials. The wide spread use of mild steel in a variety of petroleum applications, such as down hole tubular, flow lines and transmission pipelines are well known[1–[6]. Hydrochloric acid solutions are widely used in petroleum fields, for cleaning and descaling of iron and steel alloys[7–10]. The use of inhibitors is one of the best-known methods of corrosion protection[11, 12]. Organic compounds used as inhibitors act through a process of surface adsorption, so the efficiency of an inhibitor depends not only on the characteristics of the environment in which it acts, the nature of the metal surface and electrochemical potential at the interface, but also on the structure of the inhibitor itself, which includes the number of adsorption active centers in the molecule, their charge density, the molecule size, the mode of adsorption, the formation of metallic complexes and the projected area of the inhibitor on the metal surface[13–19]. The use of theoretical parameters presents two main advantages: firstly, the compounds and their various fragments and substituents can be directly characterized based on their molecular structure only; and secondly, the proposed mechanism of action can be directly accounted for in terms of the chemical reactivity of the compounds under study[20-23].

In the present paper, in order to obtain as effective inhibitor, sulfathiazole have been studied by electrochemical techniques to investigate electrochemical behaviour of mild steel in 1.0 M HCl solution. Theoretical investigation of studied compound were also described by DFT method. Fig. 1 show the molecular structure of studied inhibitor:

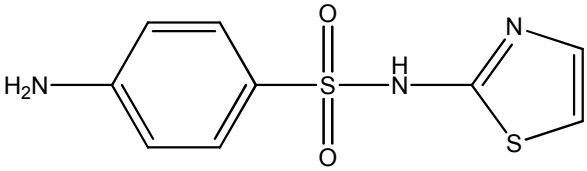

Sulfathiazole

Figure 1. Molecular structure of studied compound

MATERIALS AND METHODS

Electrodes and test solution

Corrosion tests have been performed, using the gravimetric and electrochemical measurements, on electrodes cut from sheets of carbon steel with the chemical composition: 0.370 % C, 0.230 % Si, 0.680 % Mn, 0.016 % S, 0.077 % Cr, 0.011 % Ti, 0.059 % Ni, 0.009 % Co, 0.160 % Cu, and the remainder iron.

The aggressive medium of molar hydrochloric acid used for all studies were prepared by dilution of analytical grade 37% HCl with double distilled water. The concentrations of sulfathiazole used in this investigates were varied from 10^{-4} to 5.10^{-3} M.

Gravimetric measurements

Gravimetric measurements were realized in a double walled glass cell equipped with a thermostat-cooling condenser. The carbon steel specimens used have a rectangular form with dimension of 2.5 × 2.0 × 0.2 cm were abraded with a different grade of emery paper (320-800-1200) and then washed thoroughly with distilled water and acetone. After weighing accurately, the specimens were immersed in beakers which contained 100 ml acid solutions without and with various concentrations of **STZ** at temperature equal to 303 K remained by a water thermostat for 6h as immersion time. The gravimetric tests were performed by triplicate at same conditions. The corrosion rates (C_R) and the inhibition efficiency (η_{wt}%) of carbon steel have been evaluated from mass loss measurement using the following equations:

$$C_R = \frac{w}{St} \quad (1)$$

$$\eta_{wt}\% = \frac{C_R^o - C_R}{C_R^o} \times 100 \quad (2)$$

Where w is the average weight loss before and after exposure, respectively, S is the surface area of sample, t is the exposure time, C_R^o and C_R is the corrosion rates of steel without and with the **STZ** inhibitor, respectively.

Electrochemical tests

The potentiodynamic polarization curves were conducted using an electrochemical measurement system PGZ 100 Potentiostat/Galvanostat controlled by a PC supported by the Voltamaster 4.0 Software. The electrochemical measurements were performed in a conventional three electrode glass cell with carbon steel as a working electrode, platinum as counter electrode (Pt) and a saturated calomel electrode used as a reference electrode. The working electrode surface was prepared as described above gravimetric section. Prior to each electrochemical test an immersion time of 30 min was given to allow the stabilization system at corrosion potential. The polarization curves were obtained by changing the electrode potential automatically from -800 to -200 mV/SCE at a scan rate of 1 mV s-1. The temperature is thermostatically controlled at desired temperature ±1K.The percentage protection efficiency (η_P%) is defined as:

$$\eta_P\,(\%) = \frac{I^0_{corr} - I_{corr}}{I^0_{corr}} \times 100 \quad (3)$$

Where, I^o_{corr} are corrosion current in the absence of inhibitor, I_{corr} are corrosion current in the presence of inhibitor. Electrochemical impedance spectroscopy (EIS) measurements were carried out with same equipment used for potentiodynamic polarization study (Voltalab PGZ 100) at applied sinusoidal potential waves of 5mV amplitudes with frequencies ranging from 100 KHz to 10 mHz at corrosion potential. The impedance diagrams are given in the Nyquist representation. The charge transfer resistance (Rct) was determined from Nyquist plots and double layer

capacitance (Cdl) was calculated from CPE parameters of the equivalent circuit deduced using Zview software. In this case the percentage protection efficiency (η_Z%) is can be calculated by the value of the charge transfer resistance (R_{ct})

$$\eta_z(\%) = \frac{R_{ct} - R_{ct}^0}{R_{ct}} \times 100 \quad (4)$$

WhereR_{ct}^o and R_{ct} were the polarization resistance of uninhibited and inhibited solutions, respectively.

Density Functional Theory (DFT) method

Quantum chemical method is usually used to investigate the relationship between the inhibitor molecular properties and its corrosion inhibition efficiency[23–26]. The properties include orbital energy, charge density and combined energy, etc. Some studies have investigated the correlation between the inhibitor molecular structure and its efficiency, but much less attention has been paid to simulate the adsorption mode of the inhibitor and the metal[26–28]. Quantum chemical calculations were performed using density functional theory (DFT) with the Beck's three parameter exchange functional along with the Lee-Yang-Parr non local correlation functional (B3LYP) with 6-31G (d, p) basis set is implemented in Gaussian 03 program package[29–31]. This approach is shown to yield favorable geometries for a wide variety of systems. The following quantum chemical parameters were evaluated from the optimized molecular structure: the dipole moment (μ), the energy of the highest occupied molecular orbital (E_{HOMO}), the energy of the lowest unoccupied molecular orbital (E_{LUMO}), the energy band gap ($\Delta E_{gap} = E_{HOMO} - E_{LUMO}$), the electron affinity (A), the ionization potential (I) and the number of transferred electrons (ΔN).

According to Koopman's theorem[32] the ionization potential (IE) and electron affinity (EA) of the inhibitors are calculated using the following equations.

$$IE = -E_{HOMO} \quad (5)$$

$$AE = -E_{LUMO} \quad (6)$$

Thus, the values of the electronegativity (χ) and the chemical hardness (η) according to Pearson[33], operational and approximate definitions can be evaluated using the following relations:

$$\chi = \frac{IE + EA}{2} \quad (7)$$

$$\eta = \frac{IE - EA}{2} \quad (8)$$

The number of transferred electrons (ΔN) was also calculated depending on the quantum chemical method[31], [34], [35] by using the equation:

$$\Delta N = \frac{\chi_{Fe} - \chi_{inh}}{2(\eta_{Fe} + \eta_{inh})} \quad (9)$$

Where χ_{Fe} and χ_{inh} denote the absolute electronegativity of iron and inhibitor molecule η_{Fe} and η_{inh} denote the absolute hardness of iron and the inhibitor molecule respectively. In this study, we use the theoretical value of χ_{Fe} =7.0 eV mol^{-1} and η_{Fe} = 0 eV mol^{-1}, for calculating the number of electron transferred.

RESULTS AND DISCUSSION

Polarization results

The potentiodynamic polarization curves for the mild steel in 1.0 M HCl solution in the absence and presence of different concentrations of **STZ** at 303 K are shown inFig. 2. The corrosion parameters such as corrosion potential (E_{corr}), cathodic Tafel slope (β_c) and corrosion current density (i_{corr}) obtained from these curves are given in Table 1.

Table 1. Polarization data of carbon steel in 1.0 M HCl without and with various concentrations of STZ at 303 K

Inhibitor	Conc (M)	$-E_{corr}$ (mV/SCE)	-βc (mV dec^{-1})	I_{corr} (μA cm^{-2})	η_P (%)	Θ
Blank	1.0	496	162	564.0	-	-
STZ	5.10^{-3}	501	163	30.1	94.66	0.9466
	1.10^{-3}	503	167	66.3	88.24	0.8824
	5.10^{-4}	504	156	128.4	77.23	0.7723
	1.10^{-4}	494	168	188.9	66.51	0.6651

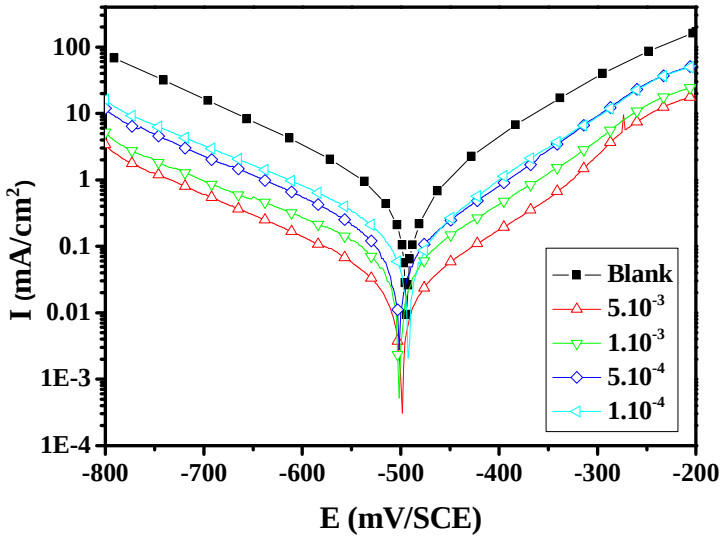

Figure 2. Polarisation curves of carbon steel in 1.0 M HCl for various concentrations of STZ at 303K

It is apparent in Fig. 2 that both anodic metal dissolution of iron and cathodic hydrogen evolution curves shifted towards lower current density after the addition of inhibitor to 1.0 M HCl solution. The lower corrosion current density (i_{corr}) values in the presence of inhibitor suggesting that the inhibitor molecule adsorbed on the surface of mild steel, thereby blocking the corrosion reaction and increasing the inhibition efficiency[36]. The value of cathodic Tafel slope slowly changed in the presence of the inhibitor as compared to the blank solution. The presence of inhibitor caused minor change in Ecorr values with respect to the Ecorr value in the absence of inhibitor. It was reported by various researchers that if the change in Ecorr value in the presence of inhibitor with respect to the Ecorr value in the absence of inhibitor is more than 85 mV, the inhibitor is recognized as an anodic or a cathodic type inhibitor whereas if the change in Ecorr value is less than 85 mV, the inhibitor is recognized as mixed type inhibitor[21, 22, 37]. A minor shift in E_{corr} values toward the negative direction was obtained in the presence of the inhibitor, indicating mixed nature of the inhibitor.

Electrochemical impedance spectroscopy measurements

Nyquist plots of mild steel in 1.0 M HCl in the presence and absence of different concentrations of **STZ** at 303 K are shown in Figure 3. All the Nyquist plots obtained were semicircle in nature and the diameter of the semicircles increases with increasing the inhibitor concentration and shape is maintained throughout the tested concentration, indicating that almost no change in the corrosion mechanism occurs due to inhibitor action. The electrochemical parameters (R_{ct}, C_{dl} and IE%) in the presence and absence of inhibitor are presented in Table 2, These parameters are calculated from the Nyquist plots by using the Equivalent circuit (Fig. 4). The introduction of CPE into the circuit was necessitated to explain the depression of the capacitance semicircle, which corresponds to surface heterogeneity resulting from surface roughness, impurities, and adsorption of inhibitor. The impedance of this element is frequency-dependent and can be calculated using the following equation:

$$Z_{CPE} = \frac{1}{Q(j\omega)^n} \quad (10)$$

Where Q is the CPE constant (in Ω^{-1} S^n cm^{-2}), ω is the angular frequency (in rad s^{-1}), j2 = -1 is the imaginary number and n is a CPE exponent which can be used as a gauge for the heterogeneity or roughness of the surface. The double layer capacitance values (C_{dl}) is evaluated from constant phase element CPE (Q, n) and a charge transfer resistance value (Rct), using the following relation:

$$C_{dl} = \sqrt[n]{Q.R_t^{1-n}} \quad (11)$$

Where Q is the constant phase element (CPE) and n is a coefficient can be used as a measure of surface inhomogeneity.

Inspection of Table 2 reveals that Rct value increase prominently while C_{dl} value tend to reduce with the increase in concentration of inhibitor.

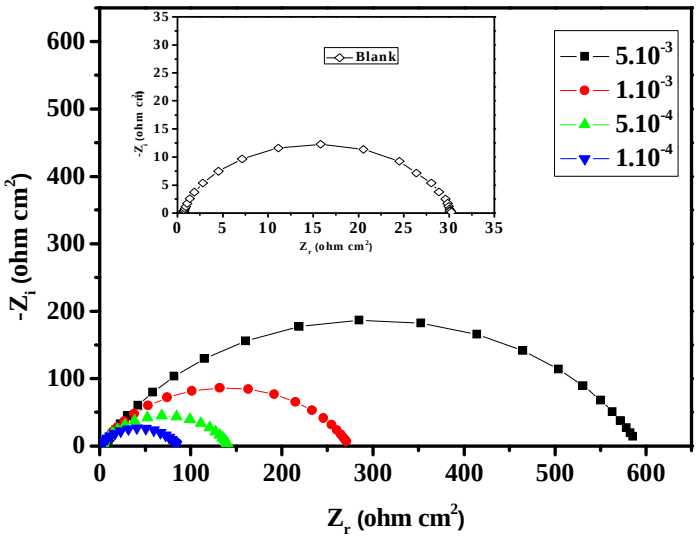

Figure 3. Nyquist diagrams for carbon steel in 1.0 M HCl containing different concentrations of STZ at 303 K

The increase in Rct value is attributed to the formation of a protective film at the metal/solution interface[24, 38, 39]. The C_{dl} value decreases on increasing the concentration of the inhibitor, indicating the decrease in local dielectric constant and/or to an increase in the thickness of the electrical double layer, suggesting that the inhibitor molecules are adsorbed at the metal/solution interface[26, 27, 40].

Table 2. Impedance parameters for corrosion of carbon steel in 1.0 M HCl in the absence and presence of different concentrations of STZat 303 K

Inhibitor	Conc (M)	R_{ct} (Ω cm^2)	n	$Q\times10^{-4}$ ($s^n\ \Omega^{-1}cm^{-2}$)	C_{dl} (μF cm^{-2})	η_z (%)	Θ
Blank	-	29 .35	0.91	1.7610	91.63	-	-
STZ	5.10^{-3}	588.5	0.8	0.1978	6.49	95.01	0.9501
	1.10^{-3}	271.4	0.82	0.3756	13.72	89.18	0.8918
	5.10^{-4}	139.1	0.82	0.8743	33.21	78.90	0.789
	1.10^{-4}	84.9	0.89	1.0978	61.59	65.43	0.6543

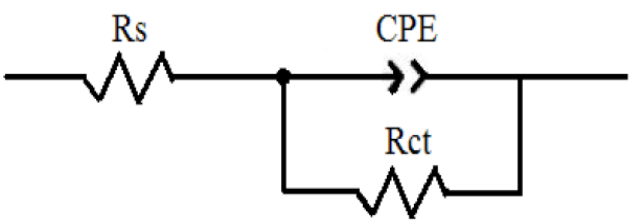

Figure 4. Equivalent electrical circuit corresponding to the corrosion process on the carbon steel in hydrochloric acid

Weight loss tests

The variation of corrosion rate (CR) with inhibitor concentration is listed in Table 3, and presented in Figure 5. It is observed that the inhibitor showed maximum inhibition efficiency (>93%) at their optimum concentration (5.10^{-3}). The excellent inhibition efficiency may be attributed to larger coverage of metal surface with inhibitor molecule. The corrosion rate decreases as the concentration of inhibitor increases.

Table 3. Corrosion parameters obtained from weight loss measurements for carbon steel in 1.0 M HCl containing various concentration of STZ at 303 K

Inhibitor	Concentration (M)	C_R (mg cm^{-2} h^{-1})	η_w (%)	Θ
Blank	-	1.135	-	-
STZ	5.10^{-3}	0.071	93.75	0.9375
	1.10^{-3}	0.144	87.34	0.8734
	5.10^{-4}	0.242	78.63	0.7863
	1.10^{-4}	0.348	69.29	0.6929

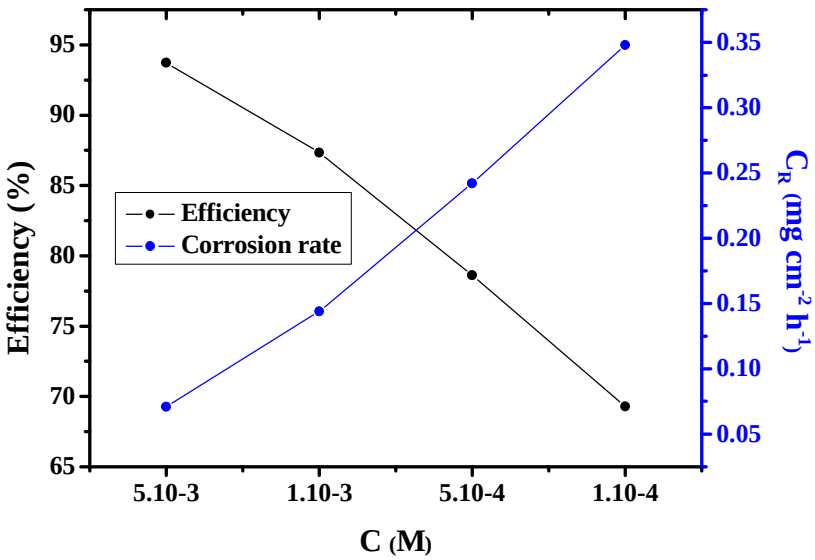

Figure 5. Relationship between the corrosion rate, the inhibition efficiency and STZ concentrations for steel after 6 h immersion in 1.0 M HCl at 303 K

Effect of temperature

In order to study the effect of temperature on the inhibition efficiency of **STZ**, polarization potentiodynamic were carried out in the temperature range 303–333 K, in the absence and in the presence of optimum concentration of inhibitor. The polarization curves are illustrated in Fig. 9and the corrosion parameter values at different temperatures are listed in Table 4. The results obtained from Polarization curves show an increase in current density and decrease in *IE*% with increasing temperature. The effect of temperature on the corrosion current (I_{corr}) can be used for determines the activation parameters for dissolution process using the Arrhenius equation and transition state equation[15, 16,41]:

$$I_{corr} = A.\exp(-\frac{E_a}{R.T}) \quad (12)$$

$$I_{corr} = \frac{RT}{Nh}.\exp\ (\frac{\Delta S^*}{R}).\exp(-\frac{\Delta H^*}{RT}) \quad (13)$$

Where E_a is the activation corrosion energy,ΔH^* is the enthalpy, ΔS^* is the entropy of activation , T is the absolute temperature in Kelvin, h is the Plank constant, N is the Avogadro number and R the molar gas constant.

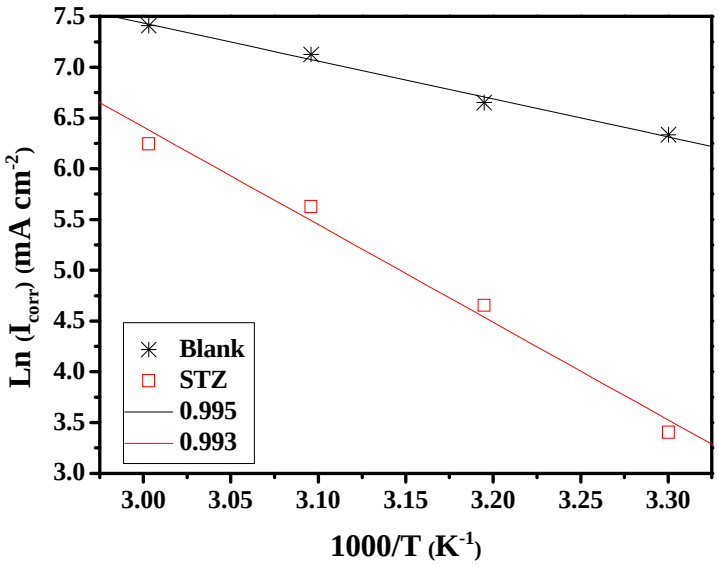

Figure 6. Arrhenius plots for mild steel in 1.0 M HCl and 1.0 M HCl + 5.10^{-3} M STZ

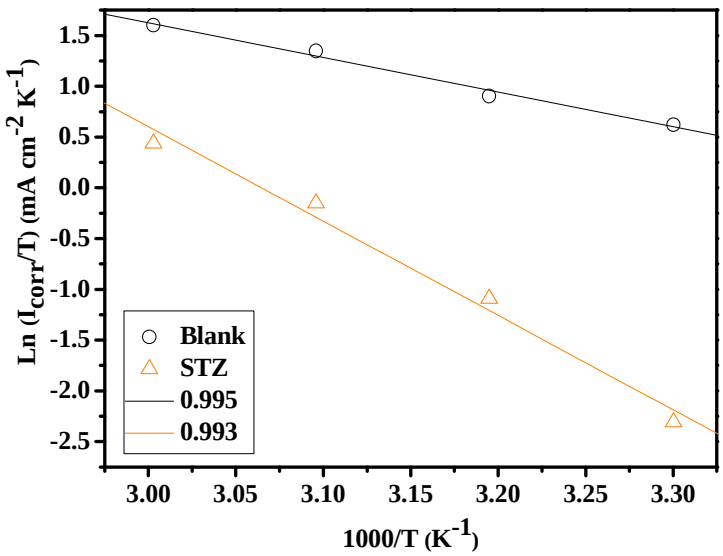

Figure 7. Transition state plots for mild steel in 1.0 M HCl and 1.0 M HCl + 5.10^{-3} MSTZ

The linear regression between ln (I_{corr}) and 1/T shown in Fig. 6 for uninhibited solution and inhibited by optimum concentration of **STZ**, we allowed to deduct the activation energy in the presence and absence of **STZ** inhibitor and the result is listed in Table 5. Calculated activation energies for the corrosion process in the absence and presence of inhibitor is given in Table 5. A decrease in inhibition efficiency with rise in temperature with analogous increase in corrosion activation energy in the presence of inhibitor compared to its absence is indicate that more energy barrier for the corrosion reaction in presence of the inhibitor is attained. Thus the adsorbed inhibitor molecules prevent charge or mass transfer from the mild steel surface[42–44].

Table 4. The influence of temperature on the electrochemical parameters for carbon steel electrode immersed in 1.0 M HCl and 1.0 M HCl + 5.10^{-3} M STZ

Inhibitor	Temp (K)	$-E_{corr}$ (mV/SCE)	$-\beta c$ (mV dec^{-1})	I_{corr} (µA cm^{-2})	η_{Tafel} (%)
Blank	303	496	162.5	564	-
	313	498	154.5	773	-
	323	492	176.0	1244	-
	333	497	192.0	1650	-
STZ	303	501	163	30.1	94.66
	313	493	167	122.5	84.15
	323	502	159	277.6	77.68
	333	496	164	466.1	71.75

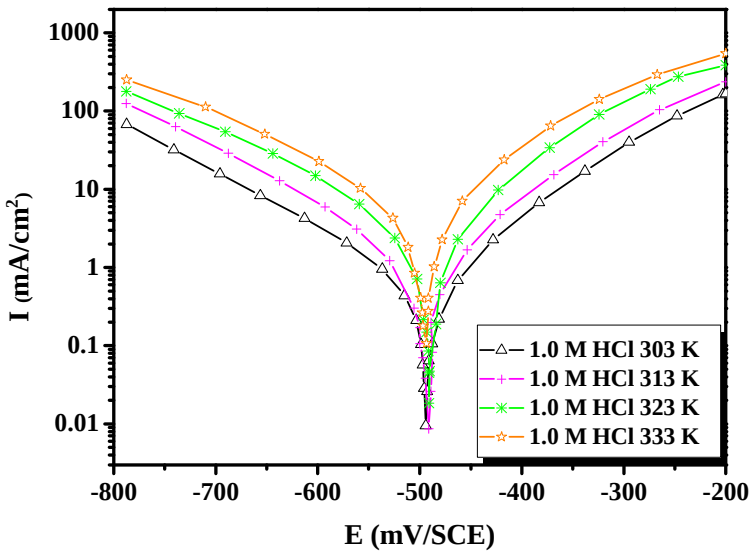

Figure 8. Potentiodynamic polarisation curves of carbon steel in 1.0 M HCl at different temperatures

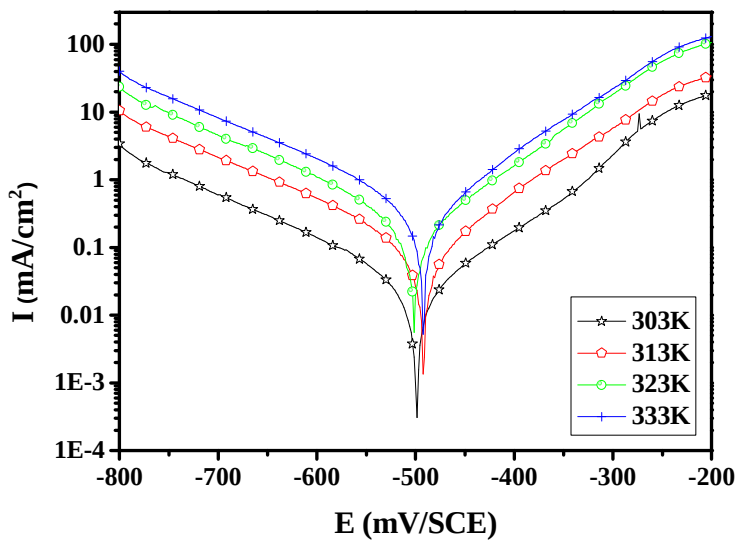

Figure 9. Potentiodynamic polarisation curves of carbon steel in 1.0 M HCl in the presence of 5.10^{-3} M STZ at different temperatures

Table 5. Corrosion kinetic parameters for mild steel in 1.0 M HCl in the presence and absence of 5.10^{-3} M STZ

Inhibitor	E_a (kJ/mol)	ΔH_a (kJ/mol)	ΔS_a (J mol-1 K-1)	$E_a - \Delta H_a$
Blank	31.00	28.35	-98.8	2.65
STZ	79.90	77.22	39.31	2.68

The values of ΔH_a and ΔS_a evaluated from the slope ($\Delta H_a/R$) and the intercept of ($\ln(R/Nh) + (\Delta S_a/R)$) of the plots of $\ln(I_{corr}/T)$ against 1/T are listed in Table 5. The positive signs of ΔH_a reflect the endothermic nature of dissolution process of the carbon steel suggesting that this dissolution is slowed. ΔS_a Value is more positive in 1.0 M HCl solution containing **STZ** as an inhibitor than that make in the uninhibited solution. Some researches explained this behavior by replacement process of water molecules during adsorption of inhibitor molecules onto the electrode surface[45–47]. The thermodynamic reaction between the Ea and ΔH_a exposed in Table 5 is verified.

Adsorption considerations

It has been assumed that organic inhibitor molecules establish their inhibition action via the adsorption of the inhibitor on to the metal surface. The adsorption process of inhibitors are influenced by the chemical structure of organic compounds, the nature and surface charge of the metal, the distribution of charge in molecule and the type of aggressive media. In general, two modes of adsorption can be considered. The proceeding of physical adsorption requires the presence of electrically charged metal surface and charged species in the bulk of the solution. Chemisorption process involves charge sharing or charge transfer from the inhibitor molecules to the metal surface[48–52]. The presence, with a transition metal having vacant low energy electron orbital, of an inhibitor molecule having relatively loosely bound electrons or hetero atoms with lone–pair electrons facilitates this adsorption.

Adsorption isotherms are very important in determining the mechanism of organic electrochemical reactions. The most frequently used adsorption isotherms are Langmuir, Temkin and Frumkin and they were tested for the description of adsorption behavior of studied compounds and was found that adsorption of inhibitor of mild steel surface in 1 M HCl solution obeys the Langmuir adsorption isotherm given by the following equation[53–55]:

$$\frac{C_{inh}}{\theta} = \frac{1}{K_{ads}} + C_{inh} \tag{14}$$

where K_{ads} designate the equilibrium constant for the adsorption process.

The proposed relation is plotted in Fig. 10. From the value of K_{ads} obtained from the Langmuir adsorption isotherm, the values of Gibb's free energy of adsorption (ΔG^o_{ads}) were calculated and are given in Table 6[56], [57].

$$\Delta G^o_{ads} = -2.303RT \log\ (55.5\ K) \tag{15}$$

where R is the universal gas constant, T is the temperature and the value of 55.5 is the concentration of water in the solution.

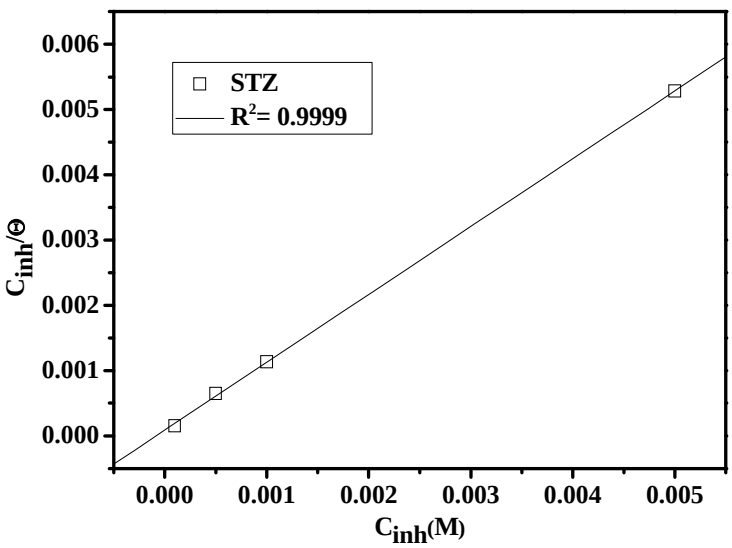

Figure 10. Langmuir adsorption of STZ on the carbon steel surface in 1.0 M HCl solution at 303K

Table 6. Thermodynamic parameters for the adsorption of STZ in 1.0 M HCl on the Carbon steel at 303K

Inhibitor	Slope	$K_{ads}(M^{-1})$	$\Delta G°_{ads}$(kJ/mol)
STZ	1.03	11400.43	-33.63

The high values of K_{ads} and negative values of $\Delta G°_{ads}$ suggest that inhibitor molecule are strongly adsorbed onto mild steel surface. The $\Delta G°_{ads}$ Value obtained for the inhibitor is −33.63 kJ mol^{-1}. This value indicate that the adsorption process of the evaluated inhibitor on the mild steel surface may involve complex interactions (both physical and chemical adsorption)[15, 16].

Quantum chemical calculation

To investigate the influence of molecular structure on corrosion inhibition capability of the **STZ**, the quantum chemical calculation were performed on the geometrically optimized **STZ** molecule (Fig. 11). Various theoretical parameters namely highest occupied molecular orbital energy (E_{HOMO}), lowest unoccupied molecular orbital energy (E_{LUMO}), dipole moment (μ) and the energy gap ΔE ($E_{LUMO} - E_{HOMO}$) were calculated from geometrically optimized neutral X molecule and used to explain their interaction with mild steel surface. The highest occupied molecular orbitals and unoccupied molecular orbitals are also called the frontier orbitals. The energy of frontier molecular orbital is a very important parameter that determines reactivity of a molecule with other chemical species. Since the E_{HOMO} is an outer most orbital (containing electron) associated with highest energy and acts as electron donor center. The E_{LUMO} is the inner most orbital having lowest energy and has capability to accept the electrons. Moreover, E_{HOMO} is an electron reach center, it is associated with the ionization potential and E_{LUMO} is an electron deficient center, it is associated with electron affinity[58–61]. The pictorial presentation of E_{HOMO} and E_{LUMO} for **STZ** molecule is shown in Fig 11. Generally, the higher value of E_{HOMO} shows that a molecule has strong tendency to donate electrons to corresponding low energy empty molecular orbitals of the acceptor molecule. The lower value of E_{LUMO} indicates that the molecule can easily accept electrons from the donor molecules[23–25].

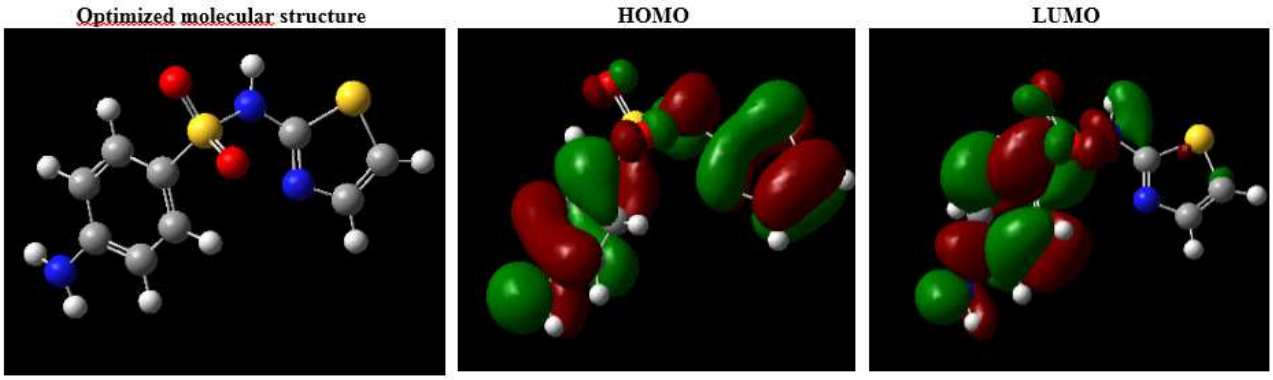

Figure 11.The optimized molecular structure and frontier molecular orbital density distributions of STZ

The calculated molecular parameters are given in Table 6. It is well studied that smaller values of ΔE ($E_{LUMO} - E_{HOMO}$) and higher value of dipole moment (μ) are responsible for enhance corrosion inhibition efficiency. The inspection of the Table 6 reveals that **STZ** has high value of E_{HOMO} and lowest value of ΔE which is obvious from its highest inhibition efficiency[20,62]. From the theoretical parameters listed in Table 6, it is also clear that **STZ**has high dipole moment (μ) which indicates that it has strongest tendency to adsorb on mild steel surface[16], [19]. These conclusions are in good agreement with the inhibition efficiency of the inhibitor obtained from weight loss, electrochemical investigations.

Table6. Quantum chemical parameters for STZ calculated using DFT/B3LYP/6-31G (d,p)

Molecular parameters	**SFMT**
E_{HOMO} (eV)	-6.16093307
E_{LUMO} (eV)	-0.92464337
ΔE_{gap} (eV)	5.2362897
μ (debye)	6.4536
I (eV)	6.16093307
A (eV)	0.92464337
χ (eV)	3.54278822
η (eV)	2.61814485
ω	16.4306241
ΔN	0.66024074
TE (a.u)	-1459.6

CONCLUSION

The weight loss and electrochemical measurements studied indicate that the **STZ** is good corrosion inhibitor for mild steel in 1 M HCl. The adsorption of the **STZ** molecule on mild steel surface was responsible for the corrosion inhibition and their adsorption on mild steel surface was according to the Langmuir adsorption isotherm. The potentiodynamic polarization study reveals that **STZ** suppressed the cathodic and anodic reactions and behaves like mixed type inhibitor. The value of ΔG_{ads} suggests that the adsorption of **STZ** on mild steel surface evolves both physical (physisorption) and chemical (chemisorption) interactions. The weight loss, electrochemical and surface studies were well supported by quantum chemical calculation study.

Acknowledgment
The authors would like to thank the Palestenian Ministry of Higher Education for their support. The support given through an "INCRECYT" research contract to M. Zougagh is also acknowledged.

REFERENCES

[1] E H A Addi, L Bazzi, M Hilali, E A Zine, R Salghi, et S E Issami, *Can. J. Chem*, **2003**, 81, 297-306.
[2] L Afia, R Salghi, L Bammou, E Bazzi, B Hammouti, L Bazzi, et A Bouyanzer, *J. Saudi Chem. Soc*, **2014**, 18, 19-25.
[3] L Afia, R Salghi, A Zarrouk, H Zarrok, E H Bazzi, B Hammouti, et M Zougagh, *Trans. Indian Inst. Met*, **2013**, 66, 43-49.
[4] L Afia, R Salghi, E H Bazzi, A Zarrouk, B Hammouti, M Bouri, H Zarrouk, L Bazzi, et L Bammou, *Res. Chem. Intermed*, **2012**, 38, 1707-1717.
[5] Anejjar A, R Salghi, A Zarrouk, O Benali, H Zarrok, B Hammouti, et E E Ebenso, *J. Assoc. Arab Univ. Basic Appl. Sci*, **2014**, 15, 21-27.
[6] Anejjar A, R Salghi, A Zarrouk, H Zarrok, O Benali, B Hammouti, S S Al-Deyab, E Benchat, et R Saddik, *Res. Chem. Intermed*, **2015**, 41, 913-925.
[7] L Bammou, M Belkhaouda, R Salghi, O Benali, A Zarrouk, H Zarrok, et B Hammouti, *J. Assoc. Arab Univ. Basic Appl. Sci*, **2014**, 16, 83-90.
[8] L Bammou, B Chebli, R Salghi, L Bazzi, B Hammouti, M Mihit, et H Idrissi, *Green Chem. Lett. Rev*, **2010**, 3, 173-178.
[9] K Barouni, L Bazzi, R Salghi, M Mihit, B Hammouti, A Albourine, et S El Issami, *Mater. Lett*, **2008**, 62, 3325-3327.
[10] L Bazzi, R Salghi, E Zine, S E Issami, S Kertit, et B Hammouti, *Can. J. Chem*, **2002**, 80, 106-112.
[11] ABousskri, A Anejjar, M Messali, R Salghi, O Benali, Y Karzazi, S Jodeh, M Zougagh, E E Ebenso, et B Hammouti, *J. Mol. Liq*, **2015**, 211, 1000-1008.
[12] O I El Mouden, A Anejjar, M Messali, R Salghi, H A Ismat, et B Hammouti, *Chem Sci Rev Lett*, **2014**, 3, 579-588.
[13] L Afia, M Larouj, H Lgaz, R Salghi, S Jodeh, S Samhan, et M Zougagh, *Der Pharma Chemica*, **2016**, 8, 22-35.
[14] ABousskri, R Salghi, A Anejjar, S Jodeh, M A Quraishi, MLarouj, H Lgaz, M Messali, S Samhan, et M Zougagh, *Der Pharma Chemica*, **2016**, 8, 67-83.
[15] BEl Makrini, M Larouj, H Lgaz, R Salghi, A Salman, M Belkhaouda, S Jodeh, M Zougagh, et H Oudda, *Der Pharma Chemica*, **2016**, 8, 227-237.
[16] BEl Makrini, H Lgaz, M Larouj, R Salghi, A Rasem Hasan, M Belkhaouda, S Jodeh, M Zougagh, et H Oudda, *Der Pharma Chemica*, **2016**, 8, 256-268.
[17] M Larouj, M Belkhaouda, H Lgaz, R Salghi, S Jodeh, S Samhan, H Serrar, S Boukhris, M Zougagh, et H Oudda, *Der Pharma Chemica*, **2016**, 8, 114-133.
[18] M Larouj, H Lgaz, S Houda, H Zarrok, H Bourazmi, A Zarrouk, A Elmidaoui, AGuenbour, S Boukhris, et H Oudda, *Journal of Materials and Environmental Science*, **2015**, 6, 3251-3267.
[19] H Lgaz, O Benali, R Salghi, S Jodeh, M Larouj, O Hamed, M Messali, S Samhan, M Zougagh, et H Oudda, *Der Pharma Chemica*, **2016**, 8, 172-190.
[20] IDanaee, O Ghasemi, G R Rashed, M Rashvand Avei, et M H Maddahy, *J. Mol. Struct*, **2013**, 1035, 247-259.
[21] D Daoud, T Douadi, H Hamani, S Chafaa, et M Al-Noaimi, *Corros. Sci*, **2015**, 94, 21-37.
[22] N O Eddy, H Momoh-Yahaya, et E E Oguzie, *J. Adv. Res*, **2015**, 6, 203-217.
[23] L Feng, H Yang, et F Wang, *Electrochimica Acta*, **2011**, 58, 427-436.
[24] H Jafari, I Danaee, H Eskandari, et M RashvandAvei, *J. Mater. Sci. Technol*, **2014**, 30, 239-252.
[25] F Kandemirli et S Sagdinc, *Corros. Sci*, **2007**, 49, 2118-2130.

[26] Khadiri, R Saddik, K Bekkouche, A Aouniti, B Hammouti, N Benchat, MBouachrine, et R Solmaz, J. Taiwan *Inst. Chem. Eng*, **2016**, 58, 552-564.
[27] F Khaled, *Electrochimica Acta*, **2010**, 55, 6523-6532.
[28] F Khaled, *Corros. Sci*, **2011**, 53, 3457-3465.
[29] J Frisch et al,Gaussian, Inc, Wallingford CT, **2004**.
[30] D Becke, *Phys. Rev. A*, **1988**, 38, 3098-3100.
[31] Lee, W Yang, et R G Parr, *Phys. Rev. B*, **1988**, 37, 785-789.
[32] R G Pearson, *Inorg. Chem*, **1988**, 27, 734–740.
[33] R G Pearson, *J. Org. Chem*, **1989**, 54, 1423–1430.
[34] X Li, S Deng, et X Xie, *Corros. Sci*, **2014**, 81, 162-175.
[35] X Li, S Deng, et X Xie, J. *Taiwan Inst. Chem. Eng*, **2014**, 45, 1865-1875.
[36] A hamad, R Prasad, et M A Quraishi, *Corros. Sci*, **2010**, 52, 1472-1481.
[37] Biswas S Pal, et G Udayabhanu, *Appl. Surf. Sci*, **2015**, 353, 173-183.
[38] V Fiori-Bimbi, P E Alvarez, H Vaca, et C A Gervasi, *Corros. Sci*, **2015**, 92, 192-199.
[39] H Hussin, A A Rahim, M N Mohamad Ibrahim, et N Brosse, *Measurement*, **2016**, 78, 90-103.
[40] S Kharchouf, L Majidi, M Bouklah, B Hammouti, A Bouyanzer, et A Aouniti, *Arab. J. Chem*, **2014**, 7, 680-686.
[41] H Lgaz, Y ELaoufir, Y Ramli, M Larouj, H Zarrok, R Salghi, A Zarrouk, A Elmidaoui, A Guenbour, E M Essassi, et H Oudda, *Der Pharma Chemica*, **2015**, 7, 36-45.
[42] B Hmamou, R Salghi, A Zarrouk, H Zarrok, R Touzani, B Hammouti, et A El Assyry, *J. Environ. Chem. Eng*, **2015**, 3, 2031-2041.
[43] B Hmamou, R Salghi, A Zarrouk, M R Aouad, O Benali, H Zarrok, M Messali, B Hammouti, M M Kabanda, et MBouachrine, *Ind. Eng. Chem. Res*, **2013**, 52, 14315-14327.
[44] DB Hmamou, R Salghi, A Zarrouk, O Benali, F Fadel, H Zarrok, et B Hammouti, *Int. J. Ind. Chem*, **2012**, 3, 1-9.
[45] D B Hmamou, R Salghi, A Zarrouk, B Hammouti, O Benali, H Zarrok, et S S Al-Deyab, *Res. Chem. Intermed*, **2013**, 39, 3475-3485.
[46] D B Hmamou, R Salghi, A Zarrouk, H Zarrok, O Benali, M Errami, et B Hammouti, *Res. Chem. Intermed*, **2013**, 39, 3291-3302.
[47] D B Hmamou, R Salghi, A Zarrouk, H Zarrouk, M Errami, B Hammouti, L Afia, L Bazzi, et L Bazzi, *Res. Chem. Intermed*, **2013**, 39, 973-989.
[48] H Zarrok, A Zarrouk, B Hammouti, R Salghi, C Jama, et F Bentiss, *Corros. Sci*, **2012**, 64, 243-252.
[49] R Salghi, M Mihit, B Hammouti, et L Bazzi, *J Iran Chem Res*, **2009**, 2, 157-162.
[50] R Salghi, L Bazzi, et M Zaafrani, *Acta Chim. Slov*, **2003**, 50, 491-504.
[51] S Patel, J Hadlicka, P Beranek, R Salghi, H Bouya, H A Ismat, et B Hammouti, *Port. Electrochimica Acta*, **2014**, 32, 395-403.
[52] M Mihit, K Laarej, H Abou El Makarim, L Bazzi, R Salghi, et B Hammouti, *Arab. J. Chem*., **2010**, 3, 55-60.
[53] M A Amin et M M Ibrahim, *Corros. Sci*, **2011**, 53, 873-885.
[54] M J Bahrami, S M A Hosseini, et P Pilvar, *Corros. Sci*, **2010**, 52, 2793-2803.
[55] D Daoud, T Douadi, S Issaadi, et S Chafaa, *Corros. Sci*, **2014**, 79, p. 50-58.
[56] Espinoza-Vázquez, G E Negrón-Silva, R González-Olvera, D Angeles-Beltrán, H Herrera-Hernández, M Romero-Romo, et M Palomar-Pardavé, *Mater. Chem. Phys*, **2014**, 145, 407-417.
[57] M H Hussin et M J Kassim, *Mater. Chem. Phys*, **2011**, 125, 461-468.
[58] N A Wazzan, *J. Ind. Eng. Chem*, **2015**, 26, 291-308.
[59] R N Singh, A Kumar, R K Tiwari, et P Rawat, *Spectrochim. Acta. A. Mol. Biomol. Spectrosc*.**2013**, 112, 182-190.
[60] L M Rodríguez-Valdez, W Villamisar, M Casales, J G González-Rodriguez, A Martínez-Villafañe, L Martinez, et D Glossman-Mitnik, *Corros. Sci*, **2006**, 48, 4053-4064.
[61] Ramya R, Mohan K, K Anupama, et A Joseph, *Mater. Chem. Phys*, **2015**, 149-150, 632-647.
[62] O Olasunkanmi, M M Kabanda, et E E Ebenso, *Phys. E Low-Dimens. Syst. Nanostructures*, **2016**, 76, 109-126.